Differential Binding of Ligands to the Apolipoprotein E Receptor 2[†]

Olav M. Andersen,*[,‡] David Benhayon,[§] Tom Curran,[§] and Thomas E. Willnow[‡]

Max-Delbrueck-Center for Molecular Medicine, Robert-Roessle-Strasse 10, D-13125 Berlin, Germany, and Department of Developmental Neurobiology, St. Jude Children's Research Hospital, 322 North Lauderdale Street, Memphis, Tennessee 38105

Received March 24, 2003; Revised Manuscript Received May 29, 2003

ABSTRACT: Apolipoprotein E receptor 2 (apoER2) is an important participant in the Reelin signaling pathway that directs cell positioning during embryogenesis. ApoER2 is a cell surface molecule that elicits intracellular signal transduction through binding of Reelin. The structural requirements for Reelin binding to apoER2 and the receptor domains involved in this process are unclear at present. Using a series of receptor mutants, we characterized the interaction of apoER2 with Reelin and compared this interaction to that of apoER2 with the receptor-associated protein (RAP), an apoER2 ligand that does not induce signaling. By surface plasmon resonance we demonstrate that apoER2 exhibits 6-fold higher affinity for Reelin than the very low density lipoprotein receptor (VLDLR), which also functions as a Reelin receptor (K_D 0.2 nM versus K_D 1.2 nM). Acidic amino acid residues in complement-type repeat domains 1 and 3 of apoER2 are required for Reelin binding. The same regions of the receptor are also bound by RAP with a 25-fold lower affinity (K_D 5 nM). Whereas RAP binds to apoER2 with a 1:1 stoichiometry, experimental evidence suggests that Reelin associates with two or more receptor molecules simultaneously to achieve high-affinity interaction. This finding indicates that aggregation of apoER2 by multivalent ligands such as Reelin may be the structural basis for signal transduction.

The low density lipoprotein (LDL)[1] receptor gene family comprises a class of cell surface receptors that share structural homology with the LDL receptor, the prototype receptor responsible for cellular uptake of lipoproteins (*1*−*3*). Members of this gene family are remarkable as they can mediate endocytosis as well as signal transduction. Some ligands such as proteinase/inhibitors or vitamin/carrier complexes are internalized by these receptors and delivered to lysosomes for degradation (*4*, *5*). However, Reelin and Wnt proteins bind to certain lipoprotein receptors on the cell surface and elicit cellular signals through adapter molecules bound to cytoplasmic domains of the receptors (*6*−*11*).

Apolipoprotein E receptor 2 (apoER2) is an example of a protein with such a dual function. In cultured cells it acts as an endocytic receptor for lipoproteins (*12*); however, in the embryonic brain it serves as a receptor for Reelin, a signaling factor that controls neuronal positioning during development (*7*, *8*). Reelin binds to apoER2 and to the related very low density lipoprotein receptor (VLDLR) on the surface of postmitotic neurons (*6*). Binding of Reelin to apoER2 and VLDLR results in tyrosine phosphorylation of specific residues of disabled-1 (Dab1), a cytosolic adapter protein associated with the cytoplasmic domain of the receptors, resulting in activation of downstream signaling pathways through the Src family of tyrosine kinases (*13*−*16*).

Almost every known ligand of LDL receptor-related receptors binds to a structural motif in the extracellular domain of the proteins known as the cluster of complement-type repeat (CR)-domains. CR-domains are 40 amino acid modules characterized by three internal disulfide bridges and a number of conserved acidic residues that form an octahedral cage around a central coordinated Ca^{2+} ion (*17*). The apoER2 cDNA encodes a cluster of eight CR-domains, not all of which are translated into the polypeptide chain. Due to alternative splicing, receptors with either four or five CR-domains are produced in vivo (*18*). Spatial and temporal differences in the expression pattern of these proteins suggest distinct physiological functions for individual receptor species (*12*, *18*−*21*).

Previously, a number of fingerprint residues with acidic side chains have been identified in CR-domains that are critical for ligand binding to the LDL receptor gene family (*22*−*25*). Surprisingly, no structural differences in the requirement for binding of ligands to apoER2 have been uncovered regardless of their downstream effects. This observation raises the question how the different extracellular ligands elicit distinct intracellular responses? To address this question, we investigated the structural requirements for ligand binding to apoER2 using two model ligands: Reelin,

[†] The present study was funded by a grant from the National Genome Research Network of the BMBF (T.E.W.) and in part by grants from the National Institutes of Health, Cancer Center Support CORE Grant P30 CA21765 (T.C.), National Institutes of Health, National Institute of Neurological Disorders and Stroke Grant RO1-NS36558 (T.C.), and American Lebanese Syrian Associated Charities (T.C.).

* Corresponding author. Tel: (+49) 30 9406 3749. Fax: (+49) 30 9406 3382. E-mail: o.andersen@mdc-berlin.de.

[‡] Max-Delbrueck-Center for Molecular Medicine.

[§] St. Jude Children's Research Hospital.

[1] Abbreviations: apoER2, apolipoprotein E receptor 2; CR-domains, complement-type repeat-domains; PCR, polymerase chain reaction; PDGF, platelet-derived growth factor; RAP, receptor-associated protein; SPR, surface plasmon resonance; LDL, low density lipoprotein; VLDLR, very low density lipoprotein receptor; LRP, LDL receptor-related protein; SDS−PAGE, sodium dodecyl sulfate−polyacrylamide gel electrophoresis; CNR, cadherin-like neuronal receptor; Dab1, disabled-1.

10.1021/bi034475p CCC: $25.00
Published on Web 07/15/2003

a signal transducing molecule, and the receptor-associated protein (RAP), an antagonist of apoER2-mediated signaling. In these studies, we present evidence that these two ligands bind to apoER2 using substantially different binding mechanisms despite the fact that they recognize overlapping binding epitopes. These different binding mechanisms may allow apoER2 to discriminate between endocytosis and signal transduction.

MATERIALS AND METHODS

Generation of ApoER2 Fragments. A cDNA construct encoding the murine apoER2 with five CR-domains (*18*) was kindly provided by T. Hiesberger (UTSW Medical Center) and served as the template for generating the various receptor fragments. Primers 5′-gcc cgc tag ccg cgg atc cgc tgc cgg gcg g-3′ and 5′-gcg gcc gct cat ggt gct cgg tag cat ttc t-3′ were used in polymerase chain reaction (PCR) to amplify a fragment spanning amino acid residues Ala^{-1} to Pro^{617} of the wild-type sequence flanked by *Nhe*I and *Not*I restriction sites. The fragment was inserted into vector pGemTeasy (Promega, www.promega.com) and verified by DNA sequencing. To produce apoER2 domains with single amino acid substitutions, a fragment including the *Nhe*I site and an internal *Bgl*II site (nucleotides 1154−1159) was removed from pGemTeasy and transferred into pEGFP-N1 (Clontech Laboratories, www.clontech.com) for site-directed mutagenesis as reported previously (*22*). The following sets of primers were used: 5′-gg aga tgc gat gag aac aac gac tgc-3′ and 5′-gca gtc gtt gtt ctc atc gca tct cc-3′ (for $Asp35^{CR1}$ to Asn), 5′-g aag tgc gac ggc cag gag gag tgt c-3′ and 5′-g aca ctc ctc ctg gcc gtc gca ctt c-3′ (for $Glu74^{CR2}$ to Gln), 5′-cgc tgc gac gga cag aag gac tgt g-3′ and 5′-c aca gtc ctt ctg tcc gtc gca gcg-3′ (for $Glu117^{CR3}$ to Gln), and 5′-cgg tgc aac cag cag cgg gac tgc-3′ and 5′-gca gtc ccg ctg ctg gtt gca ccg-3′ (for $Glu159^{CR7}$ to Gln). For multiple amino acid substitutions, the verified $Asp35^{CR1}$ to Asn mutated fragment served as the template for further mutagenesis cycles. All mutants were verified by DNA sequencing. After introduction of the base substitutions, the *Nhe*I−*Bgl*II fragment was returned to the pGemTeasy vector containing the complete *Nhe*I−*Not*I apoER2 fragment.

Protein Purifications. For production of the various receptor domains, the encoding PCR fragments were recovered by *Nhe*I and *Not*I digest from pGemTeasy and cloned into plasmid pCEP-Pu-sp-his-mys-fXa that allows expression of the proteins as carboxyl-terminal fusions with a hexahistidine tag, a myc epitope, and a factor Xa cleavage site (*26*). All constructs were introduced into 293 EBNA cells (Invitrogen, www.invitrogen.com). For purification of the wild-type apoER2 domain, conditioned medium was collected from transfected 293 EBNA cells, dialyzed against 50 mM Tris-HCl, pH 8.0, 500 mM NaCl, and 2 mM $CaCl_2$, and applied to a Ni^{2+}-charged NTA−Sepharose column at 4 °C overnight. Bound proteins were eluted in binding buffer with 450 nM imidazole, followed by buffer change to 150 mM HEPES, pH 7.4, 150 mM NaCl, 2 mM $CaCl_2$, and RAP affinity chromatography (*22*). Mutant proteins were similarly produced in 293 EBNA cells and purified by a Ni^{2+} affinity chromatography. The production of recombinant RAP from bacteria and partially purified Reelin from medium of transfected 293 cells has been reported elsewhere (*22*, *27*).

Surface Plasmon Resonance Analysis. Purified VLDLR (kindly provided by A. Nykjær, University of Aarhus) and the wild-type extracellular apoER2 domain (Hismyc-apoER2) were immobilized on CM5 BIAcore sensor chips at a surface density of 23 fmol/mm^2 using the amine coupling kit (BIAcore, www.biacore.com). Briefly, after chip activation by injection of a 1:1 mixture of 0.2 M *N*-ethyl-*N*-(3-dimethylaminopropyl)carbodiimide and 0.05 M *N*-hydroxysuccinimide, receptor-containing solutions were passed over the chip surface at 5 μL/min, followed by blocking of unused sites by 1 M ethanolamine, pH 8. Purified apoER2 mutants were diluted to a concentration of 15 μg/mL in 10 mM sodium acetate, pH 3.0, and coated in comparable densities (30−35 fmol/mm^2). All binding studies were performed in a buffer containing 10 mM HEPES, pH 7.4, 150 mM NaCl, 5 mM $CaCl_2$, 1 mM EGTA, and 0.05% Tween-20 (Ca-HBS).

For the generation of a Reelin-coated chip, partially purified Reelin enriched to an effective Reelin concentration of 100 μg/mL was passed over the activated chip surface after dilution to 20 μg/mL in 10 mM sodium acetate, pH 6.0. Injection of 443 μL of the solution resulted in the coupling of 8000 response units (RU) corresponding to 21 fmol/mm^2. As a negative control, a second flow cell with medium from mock-transfected cells was prepared. A third flow cell was coated with RAP (130 fmol/mm^2) as described before (*25*).

Before a concentration series of apoER2 domains were prepared, the mutant receptors were dialyzed against Ca-HBS for 16 h at 4 °C. The protein concentrations were measured, and identical amounts of the proteins were analyzed by 4−12% SDS−PAGE to verify comparable integrity and intensity of the protein bands. The apoER2 variants were applied to Reelin or RAP-coated surfaces at concentrations of 10, 50, 100, 200, and 400 nM in Ca-HBS that also was used as the running buffer. The dissociation of bound ligands in the presence of 150 nM soluble Hismyc-apoER2 was tested using the co-inject option that allows the immediate injection of soluble receptor fragments following the injection of either 4.5 nM Reelin or 20 nM RAP to the Hismyc-apoER2-coated biosensor chip.

Microtiter Plate Assays. For determination of ligand binding to apoER2 in microtiter wells, RAP or partially purified Reelin was iodinated using the Iodo-Gen reagent (Pierce, www.piercenet.com) according to manufacturer's protocols, yielding specific activities of 4.34×10^7 and 3.92×10^8 cpm/μg, respectively. Microtiter wells (Nunc Maxisorp, Roskilde, Denmark) were coated with various amounts of Hismyc-apoER2 by incubation for 16 h at 4 °C in 50 mM $NaHCO_3$, pH 9.6. After being blocked with 5% bovine serum albumin (BSA) for 2 h, the wells were washed with MB buffer (140 mM NaCl, 10 mM HEPES, pH 7.4, 1 mM $MgCl_2$, 2 mM $CaCl_2$) prior to incubation with ^{125}I ligands in MB buffer supplemented with 0.2% BSA for 16 h at 4 °C. Following extensive washing with MB buffer, bound radioactivity was released with 10% SDS and quantified. Nonspecific binding of the tracer to microtiter wells coated with BSA was determined in parallel and subtracted from the absolute values determined in the binding experiments.

RESULTS

To investigate the ligand binding properties of murine apoER2, we generated an eukaryotic expression construct

A

CR1 (Cys13-Thr51)	cee.dqfrc. .rnerciplv wrcdecndcs dnsde..ddc pkrt~~~~~~ ~~~	Asp35^{CR1}→Asn
CR2 (Cys52-Glu92)	cad.sdftc. .dnghciper wkcdgeeecp dgsdeskatc ssee~~~~~~ ~~~	Glu74^{CR2}→Gln
CR3 (Cys93-Pro136)	cpa.eklscg ptshkcvpas wrcdgekdce ggade..agc ptsapgp~~~ ~~~	Glu117^{CR3}→Gln
CR4	cap.hefqc. .snrsclasv fvcdgddccg dgsde..rgc sdpa~~~~~~ ~~~	
CR5	cpp.refrc. ggggtciper wvcdrqfdce drsdeaaelc gragqgttat paa	
CR6	captaqftc. .rsgecihlg wrcdgdrdck dksde..adc plgt~~~~~~ ~~~	
CR7 (Cys137-Thr176)	cre.nefqc. .gdgtcvlai krcnqerdcp dgsde..agc lqest~~~~~ ~~~	Glu159^{CR7}→Gln
CR8 (Cys177-Glu218)	cegprrfqc. .ksgecvdgg kvcddqrdcr dwsdepqkvc glne~~~~~~ ~~~	

B

	Mutation(s)	Nomenclature
NH$_2$- -COOH	Hismyc-apoER2	DEEEQ
NH$_2$- -COOH	Asp35^{CR1}→Asn	NEEEQ
NH$_2$- -COOH	Glu74^{CR2}→Gln	DQEEQ
NH$_2$- -COOH	Glu117^{CR3}→Gln	DEQEQ
NH$_2$- -COOH	Glu159^{CR7}→Gln	DEEQQ
NH$_2$- -COOH	Asp35^{CR1}→Asn, Glu74^{CR2}→Gln	NQEEQ
NH$_2$- -COOH	Asp35^{CR1}→Asn, Glu74^{CR2}→Gln, Glu117^{CR3}→Gln	NQQEQ
NH$_2$- -COOH	Asp35^{CR1}→Asn, Glu74^{CR2}→Gln, Glu117^{CR3}→Gln, Glu159^{CR7}→Gln	NQQQQ

FIGURE 1: Structure of wild-type and mutant apoER2 domains. (A) Alignment of all eight CR-domain sequences in the murine apoER2 cDNA [GenBank accession number AJ312058 (*18*)]. All CR-domain sequences were aligned so that the cysteines (bold) are conserved, as are the Ca^{2+} coordinating residues (boxed). The shaded acidic amino acids in CR1, -2, -3, and -7 were mutated to the indicated neutral residues. Amino acid residues are numbered according to Brandes et al. (*18*) when the three central CR-domains (CR4−CR6) are not included. (B) Structural representation of the wild-type extracellular apoER2 domain (Hismyc-apoER2) containing five CR-domains (CR1−3 and CR7−8) and all mutants used in this study. Boxes represent individual CR-domains, pentagons (⬠) represent the epidermal growth factor repeats, and hexagonal (⬡) clusters represent the β-propellers found in the receptor fragments. Dark boxes represent CR-domains with an acidic fingerprint side chain, and light boxes represent their neutral counterpart. (CR8 is neutral but not mutated.)

encoding the extracellular domain of the receptor fused to hexahistidine and myc epitopes (Hismyc-apoER2, Figure 1B). We chose to express the receptor variant with five CR-domains (CR1−3 and CR7−8) as this form corresponds to the splice variant predominantly observed in brain tissue (*18*). The receptor fragment was purified from transfected 293 cells and coupled to the surface of biosensor chips (see Materials and Methods for details).

Initially, we tested the binding of purified RAP and of partially purified Reelin to immobilized Hismyc-apoER2 using surface plasmon resonance (SPR) analysis (Figure 2). As a control, we employed a sensor chip containing purified VLDLR, another Reelin receptor of the LDL receptor gene family. As shown by the identical binding curves, RAP exhibited similar high-affinity interactions with Hismyc-apoER2 and VLDLR. The sensorgrams were fitted using a single binding-site model (BIAevaluation 3.1). The K_D was ~5 nM for both receptors (Table 1A). Reelin, on the other hand, bound better to Hismyc-apoER2 (K_D 0.20 nM) than to the VLDLR (K_D 1.2 nM) when the sensorgrams were fitted using the single-site binding model. The difference in affinity was due to a slower dissociation rate of the complex between Hismyc-apoER2 and Reelin (k_d 0.61×10^{-4} M s^{-1}) compared to the complex between VLDLR and Reelin (k_d 4.5×10^{-4} M s^{-1}), whereas the association rates were similar (k_a 3.1×10^5 s^{-1} and k_a 3.9×10^5 s^{-1}, respectively) (Table 2A).

Having demonstrated comparable affinities of RAP and Reelin for Hismyc-apoER2, we mapped the exact binding sites for both ligands on the receptor molecule. To accomplish this, we generated a number of receptor fragments harboring point mutations in the CR-domains. We focused on residues with acidic side chains center-positioned between Cys^{IV} and Cys^{V} of the CR-domain sequence that are thought to be critical for ligand interactions (*22*). On the basis of amino acid sequence alignments, six CR-domains in the murine apoER2 cDNA were identified that contained either an aspartic acid residue (Asp35^{CR1}) or glutamic acid residues (Glu74^{CR2}, Glu117^{CR3}, or Glu159^{CR7}) at this position (Figure 1A). Four of these CR-domains were present in the Hismyc-apoER2 polypeptide (CR1, CR2, CR3, and CR7). We substituted the negatively charged residues with their neutral counterparts (Asp→Asn and Glu→Gln) using site-directed mutagenesis. Expression vectors for the four single residue mutants Asp35^{CR1}→Asn (NEEEQ), Glu74^{CR2}→Gln (DQEEQ), Glu117^{CR3}→Gln (DEQEQ), and Glu159^{CR7}→Gln (DEEQQ) and for proteins with multiple amino acid substitutions NQEEQ, NQQEQ, and NQQQQ were generated and introduced into 293 cells. The structure and nomenclature of the mutants are indicated in Figure 1B. All mutants were efficiently produced and purified from 293 cells as shown by nonreducing SDS−polyacrylamide gel electrophoresis (SDS−PAGE) and Western blot analysis (Figure 3). Loading of equal amounts of the receptor derivatives resulted in similar staining intensity of each protein band, confirming that identical concentrations of the various mutants were used in subsequent experiments. The Hismyc tag could be removed from the receptor domains by factor Xa cleavage as shown for the wild-type Hismyc-apoER2 (Figure 3A, lane 1). Because removal of the tag did not alter the ligand binding

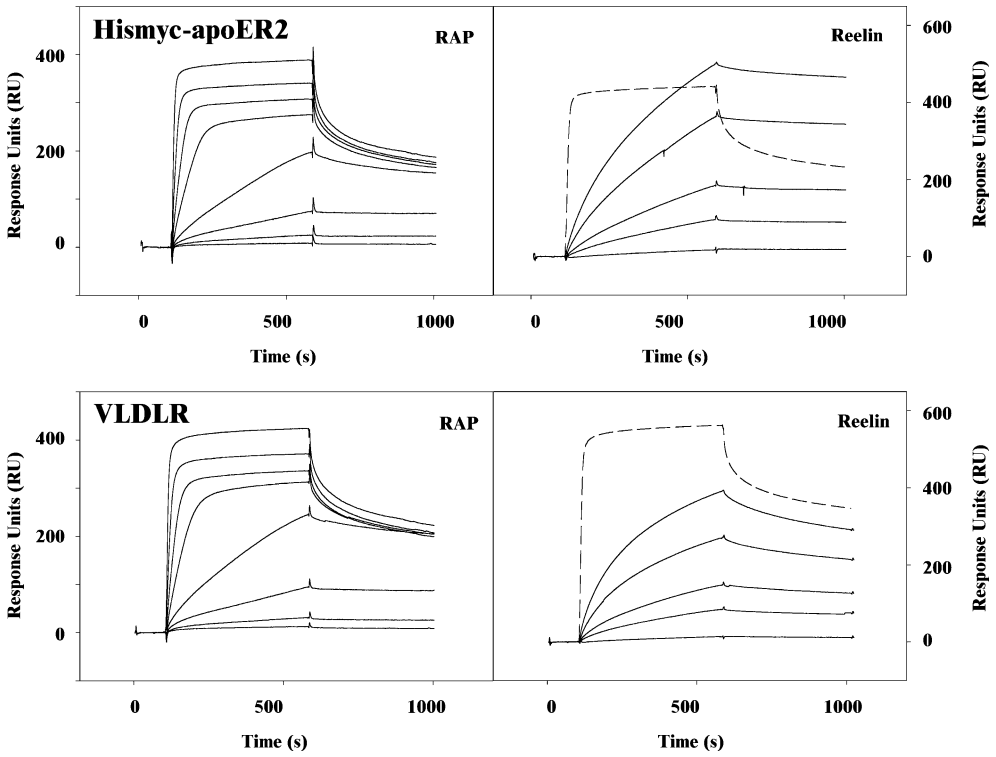

FIGURE 2: Preferred binding of Reelin to Hismyc-apoER2 compared to the VLDLR. Binding of RAP (2, 5, 10, 20, 50, 100, 200, and 500 nM) and Reelin (0.26, 1.3, 2.6, 6.5, and 13 nM) to the immobilized extracellular domains of wild-type apoER2 (upper panels) and to VLDLR (lower panels) was tested by SPR analysis. The RAP concentration series (left) showed similar binding curves for both receptors ($K_D \sim 5$ nM). For Reelin (right), a higher affinity for apoER2 (K_D 0.2 nM) than for VLDLR (K_D 1.2 nM) was apparent. For comparison, the binding curve of 1 μM RAP to the receptors (dotted line) is shown in the sensorgrams of the Reelin concentration series (solid lines).

Table 1: Kinetic Parameters for the Binding of RAP to (A) Immobilized VLDLR and Hismyc-apoER2 and to (B) Immoblized ApoER2 Mutants (Supporting Information, Figure S1)

	RAP			
	k_a (1/M s)	k_d (1/s)	K_A (1/M)	K_D (nM)
	Part A			
VLDLR	1.55×10^5	6.59×10^{-4}	2.35×10^8	4.25
apoER2	1.42×10^5	8.03×10^{-4}	1.77×10^8	5.64
	Part B			
NEEEQ	1.85×10^4	1.41×10^{-3}	1.31×10^7	76.3
DQEEQ	1.57×10^5	9.26×10^{-4}	1.70×10^8	5.88
DEQEQ	2.38×10^5	1.28×10^{-3}	1.86×10^8	5.38
DEEQQ	1.40×10^5	8.36×10^{-4}	1.68×10^8	5.96
NQEEQ	2.67×10^4	2.41×10^{-3}	1.11×10^7	90.2
NQQEQ	nd[a]	nd	nd	nd
NQQQQ	2.74×10^3	2.01×10^{-3}	1.36×10^6	733

[a] nd, not determined.

Table 2: Kinetic Parameters for Binding of Reelin to (A) Immobilized VLDLR and Hismyc-apoER2 and to (B) Immobilized ApoER2 Mutants

	Reelin			
	k_a (1/M s)	k_d (1/s)	K_A (1/M)	K_D (nM)
	Part A			
VLDLR	3.85×10^5	4.45×10^{-4}	8.65×10^8	1.16
apoER2	3.06×10^5	6.05×10^{-5}	5.06×10^9	0.20
	Part B			
NEEEQ	1.04×10^4	1.99×10^{-3}	5.23×10^6	192
DQEEQ	3.40×10^5	6.87×10^{-5}	4.95×10^9	0.20
DEQEQ	7.72×10^4	6.56×10^{-4}	1.18×10^8	8.50
DEEQQ	2.94×10^5	1.55×10^{-4}	1.90×10^9	0.53
NQEEQ	4.24×10^3	1.73×10^{-3}	2.45×10^6	409
NQQEQ	nd[a]	nd	nd	nd
NQQQQ	1.75×10^3	2.29×10^{-3}	7.64×10^5	1310

[a] nd, not determined.

properties of the receptor fragment (data not shown), tagged fusion proteins were used in following studies.

To screen all apoER2 derivatives for their ability to bind to RAP and Reelin, we prepared biosensor chips with the immobilized ligands for SPR analysis. For the interaction with RAP, we applied each apoER2 fragment to the chip surface and observed binding for some of the mutants (Figure 4A and Supporting Information, Figure S1). In particular, single amino acid substitutions DQEEQ, DEQEQ, and DEEQQ had little effect on RAP interaction, because the respective fragments bound with similar affinity as the wild-type Hismyc-apoER2 (DEEEQ) (Figure 4A). Mutation $Asp35^{CR1} \rightarrow Asn$ (NEEEQ) alone or combined with $Glu74^{CR2} \rightarrow Gln$ (NQEEQ) resulted in an intermediate affinity, whereas multiple substitutions NQQEQ and NQQQQ abolished RAP binding completely (Table 3). This finding indicated that RAP interacts preferentially with CR1 but requires the presence of at least one of the other CR-domains, because the interaction with a single CR-domain does not provide enough energy for high-affinity complex formation. The binding was modeled using either a one-site or a two-site binding mechanism, the latter represented by one high- and one moderate-affinity site (Table 3). The two-site binding model describes the binding of RAP to a fragment comprising $Asp35^{CR1}$ (the high-affinity site) and to that of a mutated CR-domain pair (the moderate-affinity site) (DQEEQ, DEQEQ, and DEEQQ), whereas the one-site model is applied for apoER2 domains containing the $Asp35^{CR1} \rightarrow Asn$ mutation. In parallel, we also tested binding of the receptor fragments to the Reelin chip. Surprisingly, neither wild-type

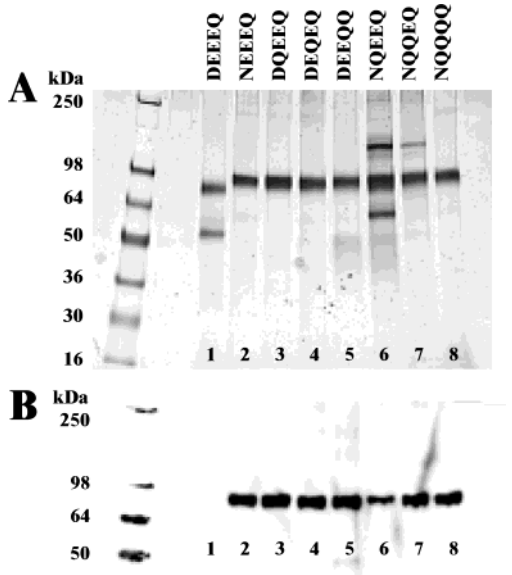

FIGURE 3: Purification of extracellular apoER2 domains. Purified apoER2 fragments containing the wild-type (Hismyc-apoER2; DEEEQ) or the indicated mutant amino acid sequences were subjected to nonreducing SDS−PAGE and (A) staining with silver nitrate (360 ng/lane) or (B) Western blot analysis using anti-hismyc antiserum (90 ng/lane). The estimated size of the Hismyc-apoER2 domains is 95 kDa. Comparable intensity and integrity of the protein bands were observed. In lane 1, the Hismyc-apoER2 domain (DEEEQ) was cleaved with factor Xa to remove the hismyc tag prior to SDS−PAGE, resulting in faster mobility of the band (panel A) and lack of detection by the antiserum (panel B) compared to the tagged mutants.

Hismyc-apoER2 nor any of the mutant fragments bound strongly to the Reelin-coated chip surface (Figure 4B). Only interactions with very low affinity due to fast off-rates were observed (Figure 4B, inset). The inability of the receptor fragments to bind was not caused by insufficient coupling of Reelin, because the CR50 antibody that recognizes functional Reelin (*28*) bound efficiently to the biosensor chip (Figure 4B).

The previous experiment demonstrated that interaction of RAP with apoER2 occurs efficiently with either of the partners immobilized on the biosensor chip. In contrast, interaction of Reelin with apoER2 required the ligand in solution. To confirm this observation, we repeated the interaction studies, this time immobilizing the individual receptor mutants. We coupled all receptor species with similar surface densities (30−35 fmol/mm^2) and tested the binding of a concentration series of RAP to the proteins (Supporting Information, Figure S2). The binding curves could be fitted to a single binding-site model with the kinetic parameters listed in Table 1B. However, this simple model could not accurately account for the binding of receptor domains to immobilized RAP (Table 3 and Supporting Information, Figure S1) where some curves fitted only to a model with two sites, one with very high and one with moderate affinity. Thus, the affinity of RAP binding to immobilized Hismyc-apoER2 (K_D ~5 nM) should in fact be taken as the mean of these two affinities (Table 1A), similar to previous observations for RAP binding to VLDLR (*29*). Again, we concluded that all single-substituted mutants were able to bind RAP with high to intermediate affinities, whereas domains with multiple mutations lacked the ability to do so. These findings support the concept that RAP

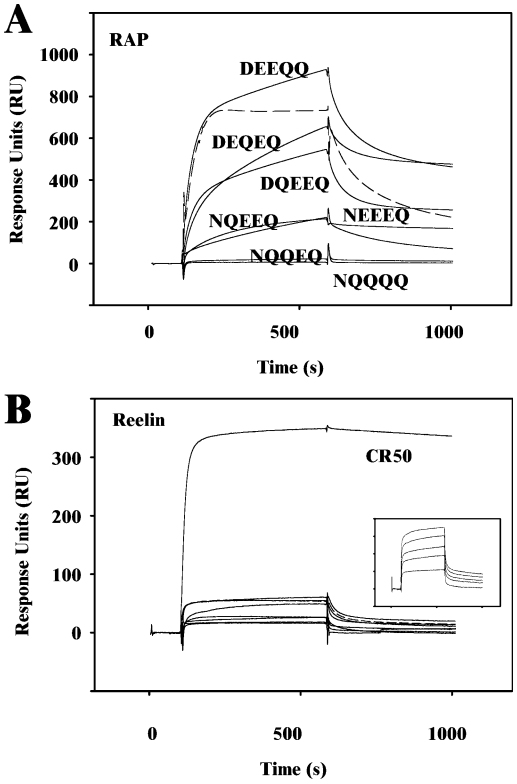

FIGURE 4: Binding of wild-type and mutant Hismyc-apoER2 derivatives to immobilized RAP and Reelin. Sensorgrams represent the binding of 200 nM wild-type (broken line) and the indicated mutant apoER2 domains (solid lines) to immobilized RAP (A) or Reelin (B). While the single amino acid-substituted domains DQEEQ, DEQEQ, DEEQQ, and NEEEQ as well as the wild-type domain (DEEEQ) bound efficiently to RAP, none of the receptor fragments bound strongly to immobilized Reelin. As a positive control, binding of the anti-Reelin antibody CR50 to the immobilized protein was also tested in panel B. The inset represents the concentration-dependent low-affinity binding of DEEEQ to Reelin with very fast observed on- and off-rates.

preferentially interacts with two adjacent CR-domains; however, the interaction was not dependent on any single CR-domain of apoER2. The RAP polypeptide is composed of three homologous domains (*25*, *30*). When all three isolated RAP domains were tested separately on the Hismyc-apoER2 chip, only the third RAP domain (amino acid residues 216−323) was able to bind (data not shown). Interestingly, the RAP domain III binding was saturable at high RAP domain III concentrations, where the molar amount of bound RAP domain III did not exceed the molar equivalent of immobilized Hismyc-apoER2, indicating a 1:1 stoichiometry of the RAP and Hismyc-apoER2 interaction (data not shown).

Next, we investigated Reelin binding to the apoER2 fragments using SPR technology. As anticipated, the interaction between Reelin and receptor took place when the ligand was in solution. Sensorgrams representing the binding of 6.5 nM Reelin to the immobilized proteins are shown in Figure 5A. To verify that the observed increase in response units was indeed specific for Reelin, we compared binding to Hismyc-apoER2 of partially purified Reelin with that of concentrated medium from mock-transfected cells (Figure 5B). No binding was detected with the latter sample, confirming the specificity of the observed signals. As shown in Figure 5A, receptor variants DQEEQ and DEEQQ

Table 3: Kinetic Parameters for the Interaction of Hismyc-apoER2 and Mutant Derivatives with Immobilized RAP (Supporting Information, Figure S2)

	RAP, moderate-affinity site				RAP, high-affinity site			
	k_{a1} (1/M s)	k_{d1} (1/s)	K_{A1} (1/M)	K_{D1} (nM)	k_{a2} (1/M s)	k_{d2} (1/s)	K_{A2} (1/M)	K_{D2} (pM)
NEEEQ[a]	1.47×10^3	1.04×10^{-4}	1.42×10^7	70.7				nb[c]
DQEEQ[b]	1.25×10^5	1.93×10^{-2}	6.58×10^6	152	8.37×10^3	7.65×10^{-7}	1.09×10^{10}	92.7
DEQEQ[b]	2.15×10^5	9.25×10^{-3}	2.32×10^7	43	1.76×10^4	1.85×10^{-6}	9.53×10^9	105
DEEQQ[b]	1.90×10^5	2.85×10^{-3}	6.66×10^7	15.0	5.31×10^3	1.55×10^{-7}	3.42×10^{10}	29.2
NQEEQ[a]	1.63×10^4	2.95×10^{-3}	5.54×10^6	181				nb
NQQEQ				nb				nb
NQQQQ				nb				nb

[a] Fitted using the 1:1 (Langmuir) binding model (BIAevaluation 3.1). [b] Fitted using the two-site binding model: heterogeneous ligand−parallel reactions (BIAevaluation 3.1). [c] nb, no binding.

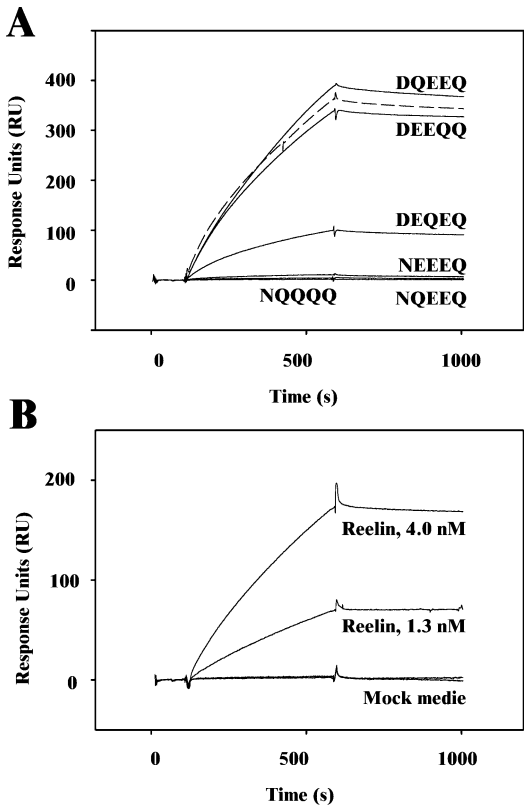

FIGURE 5: Reelin binding to immobilized apoER2 domains. (A) Sensorgrams represent the binding of 6.5 nM Reelin to flow cells coated with the indicated receptor domains (30−35 fmol/mm^2). Comparable binding was observed for the wild-type fragment (DEEEQ, broken line) and for mutants DQEEQ and DEEQQ. Partly decreased binding was seen for the mutant DEQEQ. No binding was detected for other receptor fragments. (B) Concentration-dependent binding of Reelin partly purifed from conditioned medium from Reelin-producing cells (1.3 and 4.0 nM Reelin) but not from mock-transfected cells to the DEEEQ receptor fragment.

interacted with Reelin as efficiently as the wild-type Hismyc-apoER2 fragment. Mutation of Glu117^{CR3}→Gln (DEQEQ) reduced the affinity of the interaction significantly, while all other mutations abolished binding completely. These data suggest a model whereby Reelin makes essential contact with CR1 but also recognizes CR3. Fingerprint residues in the other CR-domains were not required for Reelin to bind apoER2. These data were confirmed when the kinetic parameters were measured using a concentration series of Reelin (Table 2B).

So far, our studies demonstrated that RAP and Reelin bound to similar sites on the extracellular domain of apoER2 with similar affinities. However, a striking difference in the interaction between receptor and ligands was apparent, as the interaction of Reelin with apoER2 required the ligand to be in solution whereas the interaction between RAP and the receptor proceeded with either partner immobilized. One possible explanation for this phenomenon may be that RAP binds to apoER2 in a 1:1 stoichiometry while Reelin needs to associate with two or more receptor molecules simultaneously to achieve high-affinity interaction. Such interaction would not be possible with Reelin fixed on the biosensor chip surface and the extracellular domain of the receptor presented in solution. This model was supported by dissociation data for Reelin and RAP from Hismyc-apoER2 chips in the presence of 150 nM soluble apoER2 fragment (Figure 6). The off-rate for bound RAP from the RAP−receptor complex was increased by $\sim 2 \times 10^{-3}$ M s^{-1} in the presence of soluble apoER2 (Figure 6A). In contrast, dissociation of Reelin from Hismyc-apoER2 was only moderately affected by the soluble receptor domain with the k_d increased by $\sim 3 \times 10^{-4}$ M s^{-1}, indicating that the receptor fragment in solution did not efficiently interact with its ligand.

To confirm a higher valence binding of Reelin to Hismyc-apoER2 in an independent experimental system, we evaluated receptor and ligand interaction using a microtiter plate assay. This method has been used before to document multimeric interaction of ligands (e.g., α_2-macroglobulin) with LDL receptor-related receptors (*31*). To do so, increasing concentrations of Hismyc-apoER2 were immobilized in microtiter wells and incubated with either ^{125}I-labeled RAP or ^{125}I-labeled Reelin. Subsequently, the amount of ligands bound per well was quantified (Figure 7). In case of a 1:1 stoichiometry, the binding of ligands is independent of the receptor density in the wells and increases proportionally with the amount of receptor immobilized. For multimeric ligands that have the ability to bind to several receptor molecules simultaneously, binding is critically dependent on the receptor density. Thus, a nonlinear relationship exists between receptor concentration and ligand binding. Consistent with our hypothesis, binding of ^{125}I-RAP to Hismyc-apoER2 followed a linear relationship whereas the binding curve for ^{125}I-Reelin was nonlinear, indicative of a multivalent binding model (Figure 7).

DISCUSSION

In the present study we investigated the structural basis for ligand binding to apoER2, a receptor that plays a crucial role in signaling processes during brain development (*6*). Using two model ligands, we demonstrate that both proteins

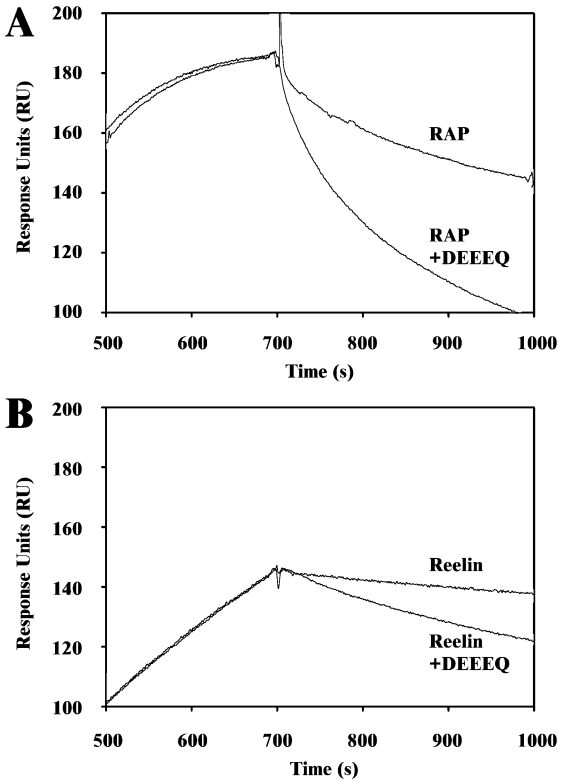

FIGURE 6: Dissociation data for (A) RAP−receptor complexes and (B) Reelin−receptor complexes in the presence or absence of soluble Hismyc-apoER2. Dissociation curves for RAP (20 nM) and Reelin (6.5 nM) binding to immobilized Hismyc-apoER2 were determined in the absence or presence of 150 nM soluble Hismyc-apoER2 fragment (+DEEEQ). The off-rate from the ligand−receptor complex for RAP was $k_d \sim 3.4 \times 10^{-3}$ M s^{-1} compared to $k_d \sim 1.4 \times 10^{-3}$ M s^{-1} in the absence of soluble apoER2. For Reelin, the dissociation rate constants were $k_d \sim 4.3 \times 10^{-4}$ M s^{-1} and $k_d \sim 1.3 \times 10^{-4}$ M s^{-1} in the presence and in the absence of soluble apoER2, respectively. A small deviation between these values and those listed in Tables 1 and 2 is due to the difference of using a local fitting procedure of a single sensorgram for a single concentration of RAP or Reelin as applied here, compared to the global fitting procedure for a series of ligand concentrations used to obtain the values in Tables 1 and 2.

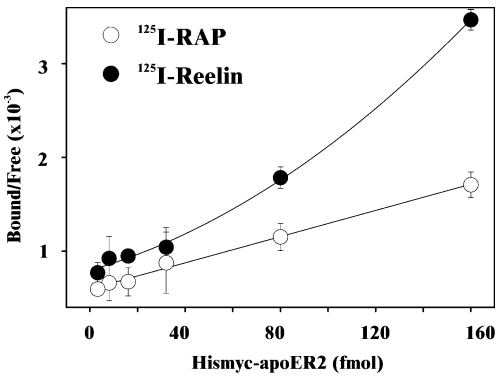

FIGURE 7: Binding of ^{125}I-RAP and ^{125}I-Reelin to Hismyc-apoER2 in microtiter wells. Increasing amounts of Hismyc-apoER2 (0−160 fmol) were immobilized in microtiter wells and incubated with 300000 cpm of ^{125}I-RAP (~1.6 nM) or ^{125}I-Reelin (~25.5 pM). Subsequently, the total amount of ligands bound to the receptors was determined. Values are means of triplicates (±SE).

bind to overlapping sites on apoER2 including the CR1. While RAP associates with the monomeric receptor in a 1:1 stoichiometric complex, experimental evidence suggests that Reelin binding may require simultaneous association with

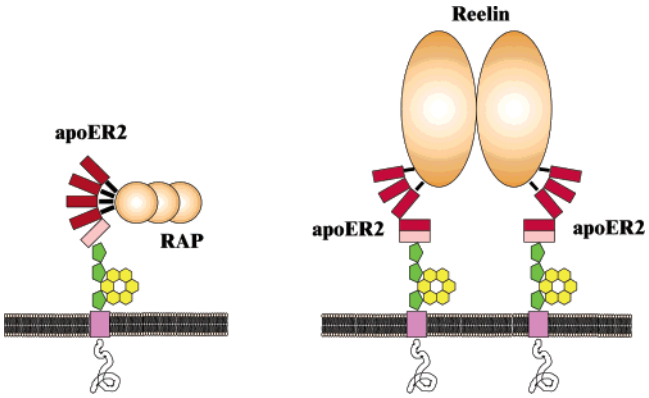

FIGURE 8: Model of RAP and Reelin binding to murine apoER2. RAP domain III exhibits the strongest affinity for CR1 but requires the interaction with at least two of the four CR-domains with acidic fingerprint residues for high-affinity binding. RAP associates with apoER2 in a 1:1 complex. Homodimeric Reelin simultaneously interacts with CR1 and CR3 in two individual receptors, causing apoER2 dimerization. Boxes represent CR-domains, pentagonals the EGF repeats, and hexagonal clusters the β-propellers in the receptor. Dark boxes represent CR-domains with an acidic fingerprint side chain.

two or more apoER2 molecules. This observation provides a possible explanation for Reelin-mediated signal transduction (but not via RAP) as it may induce receptor multimerization on the cell surface, bringing signaling factors bound to the cytoplasmic tails of the individual receptors into close proximity.

RAP is a 39 kDa protein that associates with many members of the LDL receptor gene family including apoER2 (*32*). RAP is an endoplasmatic reticulum-resident protein that associates with newly synthesized receptors and assists in their folding and intracellular transport (*33*, *34*). Because RAP blocks binding of all ligands to lipoprotein receptors, it is commonly used as a receptor antagonist in vitro, in cells, and in vivo (*32*). RAP binding inhibits receptor-mediated endocytosis of ligands as well as signal transduction (*7*, *35*−*38*). However, no cellular signaling event has been associated directly with RAP binding. Therefore, RAP provides a good model for studying apoER2-mediated ligand binding that does not induce signaling. Using site-directed mutagenesis, we mapped the binding site for RAP to the cluster of CR-domains on the receptor with Asp35^{CR1} being the major binding determinant. RAP exhibits the strongest affinity for CR1 but requires the presence of at least two adjacent CR-domains that possess an acidic fingerprint residue (Figure 8). These data agree with a previous report identifying CR-domain pairs as the minimal RAP binding unit of the LDL receptor-related protein (LRP) (*22*). The measured dissociation constant is in agreement with those reported for an apoER2 fragment containing four CR-domains (K_D 13 nM) and for LRP (K_D 7 nM) (*39*, *40*). Because only RAP domain III is able to associate with apoER2, this ligand is unlikely to physically link receptors on the cell surface (Figure 8).

Reelin is a large extracellular matrix protein with a relative molecular mass of 388 kDa. The amino-terminal protein domain contains a sequence with similarity to F-spondin, while the protein core consists of eight "Reelin repeats", each composed of approximately 370 amino acids with a central EGF-repeat motif (*41*). Reelin is produced by several populations of neurons in the developing and adult brain. During development Reelin signaling influences neuronal

positioning, axonal branching, and circuit formation by signaling through apoER2 and VLDLR on the surface of neurons (*42*, *43*). Although two members of the LDL receptor gene family, the apoER2 and the VLDLR, act as Reelin receptors, our data demonstrate that apoER2 exhibits a 6-fold higher affinity for the ligand than VLDLR, in close agreement with observations using intact cells for binding studies (*27*). Mapping studies identified $Asp35^{CR1}$ as the most dominant Reelin binding site, with an additional binding epitope located in $Glu117^{CR3}$. The fingerprint residues in CR2 and CR4 are not involved in the apoER2−Reelin interaction (Figure 8). The binding specificity of Reelin for a unique site within apoER2 is mimicked by the α_2-macroglobulin that binds to LRP with high affinity and shows a clear preference for binding to a negatively charged epitope within the fourth CR-domain of the receptor (*23*).

As evident from the lack of binding between ligand and the mutated receptor variant NQQQQ, Reelin is not able to recognize any receptor motif other than the CR-cluster. This finding is important in the context of previous data showing that other signaling molecules such as Wnt and Dickkopf bind to EGF-precursor homology domains rather than the CR-domains (*44*, *45*). The similar observation for RAP may explain the need of the additional chaperone for folding of receptor domains other than the CR-clusters (such as Boca/Mesd for the β-propellers) (*45*, *46*).

It is noteworthy that apoER2−ligand binding is critically dependent on ionic interaction between the acidic fingerprint residues and ligands as in the case of LRP (*22*, *25*). Besides the direct role in ligand recognition, these residues also play a pivotal function in the intramolecular rearrangement upon the decrease in pH within endosomes, a mechanism that results in the release of bound ligands (*46*).

Perhaps the most surprising finding when studying Reelin and apoER2 interaction is the hypothesis that Reelin may not be able to bind efficiently to monomeric receptors but requires multivalent association with two or more receptor molecules. This hypothesis is based on the fact that soluble receptors are not able to associate with immobilized Reelin and do not efficiently dissociate the ligand from a preformed receptor complex. The effect of soluble receptor domains on the dissociation phase of immobilized receptor−RAP complexes and immobilized receptor−Reelin complexes strongly resembles the SPR data collected for the release of monomeric and dimeric ligands, respectively, studying the interactions between antibodies and carbohydrates (*47*). Further support for this model stems from the fact that binding of Reelin to apoER2 in microtiter wells is critically dependent on receptor density, a phenomenon typically observed for multivalent ligands of the LDL receptor gene family. Although some technical difficulties may affect individual studies, cumulative evidence from three independent experimental setups supports the concept of a multivalent interaction between Reelin and apoER2.

Previously, it was suggested that simultaneous binding of ligands to several receptors on the cell surface triggers signal transduction by bringing into close proximity intracellular factors bound to the receptor tails causing phosphorylation of Dab1 (*1*). Our studies provide biochemical evidence supporting the notion that Reelin-mediated cross-linking of receptors is essential for the signaling factor to achieve a high-affinity interaction with its receptor. Thus, binding of Reelin to apoER2 in vivo will result in the formation of homomeric receptor complexes. Whether such receptor complexes can also include heteromeric complexes of apoER2 and VLDLR remains to be shown. An essential role of ligand-induced receptor aggregation is supported by recent findings that Reelin in solution is a dimer and that Reelin lacking the multimerization domain is functionally inactive (*48*, *49*).

Ever since signaling through LRPs was uncovered, it remained a puzzle how various ligands binding to overlapping sites in the CR-domains elicit distinct cellular responses even when acting on the same cell type. For example, RAP binding to apoER2 blocks long-term potentiation induction whereas Reelin caused a trend toward enhanced long-term potentiation induction (*50*). Based on our findings, it is tempting to speculate that the ability of individual ligands to dimerize receptors may provide the structural basis for distinct cellular responses. In the simplest model, monovalent ligands such as vitamin carriers, proteinase inhibitors, or RAP are substrates for receptor-mediated endocytosis and lysosomal catabolism. Multivalent ligands such as Reelin, on the other hand, may cause receptor aggregation and signal transduction. In support of this hypothesis, several multivalent ligands have been shown to induce signaling through LRP. These ligands include platelet-derived growth factor (PDGF) and α_2-macroglobulin. Binding of PDGF homodimers to LRP activates downstream signaling via the PDGF receptor and Src-mediated phosphorylation of the LRP tail (*38*, *51*). Tetrameric α_2-macroglobulin regulates Ca^{2+} signaling via linkage of LRP to *N*-methyl-D-aspartate receptors (*36*, *51*).

ACKNOWLEDGMENT

We thank H. Schultz, G. Wrettos, and M. Eigen for expert technical assistance and A. Nykjær, T. Hiesberger, and G. Burmeister for sharing reagents.

SUPPORTING INFORMATION AVAILABLE

Figures showing the concentration-dependent binding of all the mutated apoER2 domains to immobilized RAP, as well as the concentration-dependent binding of RAP to each immobilized Hismyc-apoER2 mutant. This material is available free of charge via the Internet at http://pubs.acs.org.

REFERENCES

1. Willnow, T. E., Nykjær, A., and Herz, J. (1999) Lipoprotein receptors: new roles for ancient proteins, *Nat. Cell Biol. 1*, E157−E162.
2. Herz, J. (2001) The LDL receptor gene family: (un)expected signal transducers in the brain, *Neuron 29*, 571−581.
3. Nykjær, A., and Willnow, T. E. (2002) The low-density lipoprotein receptor gene family: a cellular Swiss army knife?, *Trends Cell Biol. 12*, 273−280.
4. Nykjær, A., Petersen, C. M., Møller, B., Jensen, P. H., Moestrup, S. K., Holtet, T. L., Etzerodt, M., Thøgersen, H. C., Munch, M., Andreasen, P. A., and Gliemann, J. (1992) Purified α_2-macroglobulin receptor/LDL receptor-related protein binds urokinase-.plasminogen activator inhibitor type-1 complex. Evidence that the α_2-macroglobulin receptor mediates cellular degradation of urokinase receptor-bound complexes, *J. Biol. Chem. 267*, 14543−14546.
5. Nykjær, A., Dragun, D., Walther, D., Vorum, H., Jacobsen, C., Herz, J., Melsen, F., Christensen, E. I., and Willnow, T. E. (1999) An endocytic pathway essential for renal uptake and activation of the steroid 25-(OH) vitamin D_3, *Cell 96*, 507−515.

6. Trommsdorff, M., Gotthardt, M., Hiesberger, T., Shelton, J., Stockinger, W., Nimpf, J., Hammer, R. E., Richardson, J. A., and Herz, J. (1999) Reeler/Disabled-like disruption of neuronal migration in knockout mice lacking the VLDL receptor and ApoE receptor 2, *Cell 97*, 689−701.
7. D'Arcangelo, G., Homayouni, R., Keshvara, L., Rice, D. S., Sheldon, M., and Curran, T. (1999) Reelin is a ligand for lipoprotein receptors, *Neuron 24*, 471−479.
8. Hiesberger, T., Trommsdorff, M., Howell, B. W., Goffinet, A., Mumby, M. C., Cooper, J. A., and Herz, J. (1999) Direct binding of Reelin to VLDL receptor and ApoE receptor 2 induces tyrosine phosphorylation of disabled-1 and modulates tau phosphorylation, *Neuron 24*, 481−489.
9. Pinson, K. I., Brennan, J., Monkley, S., Avery, B. J., and Skarnes, W. C. (2000) An LDL-receptor-related protein mediates Wnt signaling in mice, *Nature 407*, 535−538.
10. Tamai, K., Semenov, M., Kato, Y., Spokony, R., Liu, C., Katsuyama, Y., Hess, F., Saint-Jeannet, J.-P., and He, X. (2000) LDL-receptor-related proteins in Wnt signal transduction, *Nature 407*, 530−535.
11. Wehrli, M., Dougan, S. T., Caldwell, K., O'Keefe, L., Schwartz, S., Vaizel-Ohayon, D., Schejter, E., Tomlinson, A., and DiNardo, S. (2000) *arrow* encodes an LDL-receptor-related protein essential for Wingless signaling, *Nature 407*, 527−530.
12. Kim, D.-H., Iijima, H., Goto, K., Sakai, J., Ishii, H., Kim, H.-J., Suzuki, H., Kondo, H., Saeki, S., and Yamamoto, T. (1996) Human apolipoprotein E receptor 2. A novel lipoprotein receptor of the low density lipoprotein receptor family predominantly expressed in brain, *J. Biol. Chem. 271*, 8373−8380.
13. Trommsdorff, M., Borg, J.-P., Margolis, B., and Herz, J. (1998) Interaction of cytosolic adaptor proteins with neuronal apolipoprotein E receptors and the amyloid precursor protein, *J. Biol. Chem. 273*, 33556−33560.
14. Keshvara, L., Benhayon, D., Magdaleno, S., and Curran, T. (2001) Identification of reelin-induced sites of tyrosyl phosphorylation on disabled 1, *J. Biol. Chem. 276*, 16008−16014.
15. Arnaud, L., Ballif, B. A., Forster, E., and Cooper, J. A. (2003) Fyn tyrosine kinase is a critical regulator of disabled-1 during brain development, *Curr. Biol. 13*, 9−17.
16. Bock, H. H., and Herz, J. (2003) Reelin activates SRC family tyrosine kinases in neurons, *Curr. Biol. 13*, 18−26.
17. Fass, D., Blacklow, S., Kim, P. S., and Berger, J. M. (1997) Molecular basis of familial hypercholesterolaemia from structure of LDL receptor module, *Nature 388*, 691−693.
18. Brandes, C., Kahr, L., Stockinger, W., Hiesberger, T., Schneider, W. J., and Nimpf, J. (2001) Alternative splicing in the ligand binding domain of mouse apoE receptor-2 produces receptor variants binding reelin but not α_2-macroglobulin, *J. Biol. Chem. 276*, 22160−22169.
19. Kim, D.-H., Magoori, K., Inoue, T. R., Mao, C. C., Kim, H.-J., Suzuki, H., Fujita, T., Endo, Y., Saeki, S., and Yamamoto, T. T. (1997) Exon/intron organization, chromosome localization, alternative splicing, and transcription units of the human apolipoprotein E receptor 2 gene, *J. Biol. Chem. 272*, 8498−8504.
20. Sun, X.-M., and Soutar, A. K. (1999) Expression in vitro of alternatively spliced variants of the messenger RNA for human apolipoprotein E receptor-2 identified in human tissues by ribonuclease protection assays, *Eur. J. Biochem. 262*, 230−239.
21. Korschineck, I., Ziegler, S., Breuss, J., Lang, I., Lorenz, M., Kaun, C., Ambros, P. F., and Binder, B. R. (2001) Identification of a novel exon in apolipoprotein E receptor 2 leading to alternatively spliced mRNAs found in cells of the vascular wall but not in neuronal tissue, *J. Biol. Chem. 276*, 13192−13197.
22. Andersen, O. M., Christensen, L. L., Christensen, P. A., Sørensen, E. S., Jacobsen, C., Moestrup, S. K., Etzerodt, M., and Thøgersen, H. C. (2000) Identification of the minimal functional unit in the low-density lipoprotein receptor-related protein for binding the receptor-associated protein (RAP), *J. Biol. Chem. 275*, 21017−21024.
23. Andersen, O. M., Christensen, P. A., Christensen, L. L., Jacobsen, C., Moestrup, S. K., Etzerodt, M., and Thøgersen, H. C. (2000) Specific binding of α-macroglobulin to complement-type repeat CR4 of the low-density lipoprotein receptor-related protein, *Biochemistry 39*, 10627−10633.
24. Andersen, O. M., Petersen, H. H., Jacobsen, C., Moestrup, S. K., Etzerodt, M., Andreasen, P. A., and Thøgersen, H. C. (2001) Analysis of a two-domain binding site for the urokinase-type plasminogen activator−plasminogen activator inhibitor-1 complex in low-density lipoprotein receptor-related protein, *Biochem. J.*, 289−296.
25. Andersen, O. M., Schwarz, F. P., Eisenstein, E., Jacobsen, C., Moestrup, S. K., Etzerodt, M., and Thøgersen, H. C. (2001) Dominant thermodynamic role of the third independent receptor binding site in the receptor-associated protein RAP, *Biochemistry 40*, 15408−15417.
26. Hilpert, J., Vorum, H., Burmeister, R., Spoelgen, R., Grishkovskaya, I., Misselwitz, R., Nykjaer, A., and Willnow, T. E. (2001) Efficient eukaryotic expression system for authentic human sex hormone-binding globulin, *Biochem. J. 360*, 609−615.
27. Benhayon, D., Magdaleno, S., and Curran, T. (2003) Reelin-induced tyrosine phosphorylation of disabled-1 is mediated by apoER2 and VLDLR, *Mol. Brain Res. 112*, 33−45.
28. D'Arcangelo, G., Nakajima, K., Miyata, T., Ogawa, M., Mikoshiba, K., and Curran, T. (1997) Reelin is a secreted glycoprotein recognized by the CR-50 monoclonal antibody, *J. Neurosci. 17*, 23−31.
29. Rettenberger, P. M., Oka, K., Ellgaard, L., Petersen, H. H., Christensen, A., Martensen, P. M., Monard, D., Etzerodt, M., Chan, L., and Andreasen, P. A. (1999) Ligand binding properties of the very low-density lipoprotein receptor. Absence of the third complement-type repeat encoded by exon 4 is associated with reduced binding of Mr 40,000 receptor-associated protein, *J. Biol. Chem. 274*, 8973−8980.
30. Ellgaard, L., Holtet, T. L., Nielsen, P. R., Etzerodt, M., Gliemann, J., and Thøgersen, H. C. (1997) Dissection of the domain architecture of the alpha2macroglobulin-receptor-associated protein, *Eur. J. Biochem. 244*, 544−551.
31. Moestrup, S. K., and Gliemann, J. (1991) Analysis of ligand recognition by the purified α_2-macroglobulin receptor (low-density lipoprotein receptor-related protein). Evidence that high affinity of α_2-macroglobulin−proteinase complex is achieved by binding to adjacent receptors, *J. Biol. Chem. 266*, 14011−14017.
32. Bu, G. (2001) The roles of receptor-associated protein (RAP) as a molecular chaperone for members of the LDL receptor family, *Int. Rev. Cytol. 209*, 79−116.
33. Willnow, T. E., Armstrong, S. A., Hammer, R. E., and Herz, J. (1995) Functional expression of low-density lipoprotein receptor-related protein is controlled by receptor-associated protein *in vivo*, *Proc. Natl. Acad. Sci. U.S.A. 92*, 4537−4541.
34. Willnow, T. E., Rohlmann, A., Horton, J., Otani, H., Braun, J. R., Hammer, R. E., and Herz, J. (1996) RAP, a specialized chaperone, prevents ligand-induced ER retention and degradation of LDL receptor-related endocytic receptors, *EMBO J. 15*, 2632−2639.
35. Goretzki, L., and Mueller, B. M. (1998) Low-density-lipoprotein-receptor-related protein (LRP) interacts with a GTP-binding protein, *Biochem. J. 336*, 381−386.
36. Bacskai, B. J., Xia, M. Q., Strickland, D. K., Rebeck, G. W., and Hyman, B. T. (2000) The endocytic receptor protein LRP also mediates neuronal calcium signaling via *N*-methyl-D-aspartate receptors, *Proc. Natl. Acad. Sci. U.S.A. 97*, 11551−11556.
37. Beffert, U., Morfini, G., Bock, H. H., Reyna, H., Brady, S. T., and Herz, J. (2002) Reelin-mediated signaling locally regulates PKB/Akt and GSK-3β, *J. Biol. Chem. 277*, 49958−49964.
38. Boucher, P., Liu, P., Gotthardt, M., Hiesberger, T., Anderson, R. G., and Herz, J. (2002) Platelet-derived growth factor mediates tyrosine phosphorylation of the cytoplasmic domain of the low-density lipoprotein receptor-related protein in caveolae, *J. Biol. Chem. 277*, 15507−15513.
39. Koch, S., Strasser, V., Hauser, C., Fasching, D., Brandes, C., Bajari, T. M., Schneider, W. J., and Nimpf, J. (2002) A secreted soluble form of apoE receptor 2 acts as a dominant-negative receptor and inhibits reelin signaling, *EMBO J. 21*, 5996−6004.
40. Medved, L. V., Migliorini, M., Mikhailenko, I., Barrientos, L. G., Llinás, M., and Strickland, D. K. (1999) Domain organization of the 39-kDa receptor-associated protein, *J. Biol. Chem. 274*, 717−727.
41. D'Arcangelo, G., Miao, G. G., Chen, S.-C., Soares, H. D., Morgan, J. I., and Curran, T. (1995) A protein related to extracellular matrix proteins deleted in the mouse mutant *reeler*, *Nature 374*, 719−723.
42. Rice, D. S., and Curran, T. (2001) Role of the reelin signaling pathway in central nervous system development, *Annu. Rev. Neurosci. 24*, 1005−1039.
43. Herz, J., and Bock, H. H. (2002) Lipoprotein receptors in the nervous system, *Annu. Rev. Biochem. 71*, 405−434.

44. Mao, J., Wang, J., Liu, B., Pan, W., Farr, G. H., III, Flynn, C., Yuan, H., Takada, S., Kimelman, D., Li, L., and Wu, D. (2001) Low-density lipoprotein receptor-related protein-5 binds to Axin and regulates the canonical Wnt signaling pathway, *Mol. Cell 7*, 801−809.
45. Mao, B., Wu, W., Li, Y., Hoppe, D., Stannek, P., Glinka, A., and Niehrs, C. (2001) LDL-receptor-related protein 6 is a receptor for Dickkopf proteins, *Nature 411*, 321−325.
46. Rudenko, G., Henry, L., Henderson, K., Ichtchenko, K., Brown, M. S., Goldstein, J. L., and Deisenhofer, J. (2002) Structure of the LDL receptor extracellular domain at endosomal pH, *Science 298*, 2353−2358.
47. MacKenzie, C. R., Hirama, T., Deng, S. J., Bundle, D. R., Narang, S. A., and Young, N. M. (1996) Analysis by surface plasmon resonance of the influence of valence on the ligand binding affinity and kinetics of an anti-carbohydrate antibody, *J. Biol. Chem. 271*, 1527−1533.
48. Kubo, K., Mikoshiba, K., and Nakajima, K. (2002) Secreted reelin molecules form homodimers, *Neurosci. Res. 43*, 381−388.
49. Utsunomiya-Tate, N., Kubo, K., Tate, S., Kainosho, M., Katayama, E., Nakajima, K., and Mikoshiba, K. (2000) Reelin molecules assemble together to form a large protein complex, which is inhibited by the function-blocking CR-50 antibody, *Proc. Natl. Acad. Sci. U.S.A. 97*, 9729−9734.
50. Weeber, E. J., Beffert, U., Jones, C., Christian, J. M., Förster, E., Sweatt, J. D., and Herz, J. (2002) Reelin and ApoE receptors cooperate to enhance hippocampal synaptic plasticity and learning, *J. Biol. Chem. 277*, 39944−39952.
51. Qiu, Z., Strickland, D. K., Hyman, B. T., and Rebeck, G. W. (2002) α_2-Macroglobulin exposure reduces calcium responses to *N*-methyl-D-aspartate via low-density lipoprotein receptor-related protein in cultured hippocampal neurons, *J. Biol. Chem. 277*, 14458−14466.

BI034475P